American Mineralogist, Volume 61, pages 603–615, 1976

Single-pyroxene geothermometry and geobarometry

JEAN-CLAUDE C. MERCIER

Department of Earth and Space Sciences, State University of New York
Stony Brook, New York 11794

Abstract

The available experimental data for the equilibrium reactions that characterize either the enstatite–diopside join or the Al-concentration in pyroxenes coexisting with an Al-rich phase are reduced to three or four thermodynamic constants, entropy, enthalpy, and change in volume (two parameters for the En/Di join). Used together with a set of partition coefficients derived from natural assemblages, these values allow independent estimates of pressure and temperature to be made for any single pyroxene phase in equilibrium with a second pyroxene and with either spinel or garnet; otherwise, minimum temperatures and maximum pressures are obtained. This method has been checked for consistency both internally (similar estimates for coexisting pyroxenes in equilibrium) and externally (agreement with independent observations).

The geothermometers and geobarometers are applied to xenoliths from "kimberlites" of the Navajo Indian Reservation and to ophiolites from Western Newfoundland, for both of which partial recrystallization into hydrous phases often prevented the use of any other technique. This method is also applied to determine pressure–temperature paths for partially reequilibrated textures, to derive pyroxene geotherms from xenocrysts, to detect disequilibrium between coexisting pyroxenes, and to reveal actual equilibration facies of complex parageneses. These studies support (1) a remarkable shortening of Newfoundland ophiolitic sequences, originally 100 km thick, (2) a shallow origin for the Navajo Reservation "kimberlites," and (3) an underthrusting of oceanic-type lithosphere beneath the western United States' crust.

Introduction

Pyroxene geothermometry and geobarometry have become fundamental in determining, as a function of depth, the petrological character and structural state of the earth's upper mantle. There are, however, many important instances in which only one pyroxene phase is chemically known, precluding direct application of the classical methods. Provided that this phase was originally in equilibrium with a second pyroxene and an Al-phase, its temperature and pressure at equilibration may be calculated on the basis of thermodynamic parameters determined from experimental data, and partitioning coefficients determined empirically from natural assemblages.

Experimental data and theoretical derivations pertinent to the enstatite–diopside join and to Al-concentrations in pyroxenes in equilibrium with an Al-rich phase (spinel or garnet) have been reviewed recently by Boettcher (1974) and Mercier and Carter (1975), and these data have been used to compute a series of parameters (enthalpy, entropy, and change in volume) which completely describe a given system within the precision of the data (Mercier and Carter, 1975). A set of equations is derived here which allows a computation of fully corrected pressure and temperature estimates from the composition of either pyroxene phase, provided that this phase has been in equilibrium with another pyroxene and an Al-rich phase; otherwise, the estimates obtained are only minimum temperatures and maximum pressures. In addition to the thermodynamic parameters referred to above, these equations contain a set of partition coefficients derived from hundreds of natural assemblages. Written in this way, any refinement of the experimental data can be easily taken into account through replacement of the constant(s) affected.

The single-pyroxene technique is first tested on texturally equilibrated metamorphic lherzolites, also

assumed to be chemically equilibrated, to determine the uncertainty related to the analyses used. This is achieved by deriving independently pressure and temperature estimates for each pyroxene phase in various samples. Whereas the experimental data used to compute the thermodynamic parameters for the enstatite/diopside solvus and for the Al solubility in pyroxenes (garnet facies) are generally accepted, data on the Al solubility in pure enstatite for the spinel facies are still controversial. MacGregor's (1974) isopleths are accepted as a realistic model for the average natural pyroxene compositions (Mercier and Carter, 1975), and the validity of such a model is confirmed by the agreement between maximum and minimum depths of extension of the spinel facies, derived for several localities from (1) the model based on MacGregor's data, and (2) geophysical data for the Moho. and/or the shallowest garnet lherzolites recognized.

Inclusions in the diatremes in the Navajo Indian Reservation (Utah–Arizona) and ophiolites from Newfoundland are discussed here as two applications of the single-pyroxene technique, since low-temperature transformations (serpentinization, chloritization, *etc* . . .) and recrystallization had left a few remnants of only one of the original pyroxene phases in most of the samples. Pyroxene xenocrysts from the Navajo Reservation diatremes have also been included in the study.

The method

The general method for fitting the available experimental data and for extrapolation of the results from a given pyroxene phase to the other has been recently discussed by Mercier and Carter (1975). The method described here emphasizes the possibility of deriving fully corrected temperature and pressure estimates from any single analysis of a pyroxene provided (or assuming) an original equilibrium with a second pyroxene and an Al-phase (spinel or garnet). Although the parageneses used should also contain olivine (reaction given below), the equations might apply to some olivine-free assemblages, since no significant differences are found for estimates derived from peridotites and coexisting reequilibrated pyroxenites (recrystallized tectonites). In experiments, the enstatite/diopside join, at least, seems insensitive to the degree of Si saturation (Lindsley and Dixon, 1976). However, many pyroxenites still have magmatic textures and therefore the estimates derived from them cannot be representative of regional conditions.

Derivation of the equations

The classical pressure equation

$$P = (RT\ln K' + T\Delta S - \Delta H)/\Delta V$$

has been used to fit K' composition-isopleths in P-T space (Mercier and Carter, 1975) and to derive enthalpy, entropy, and change-in-volume values for the equilibrium reactions related to the enstatite/diopside join

$$\underset{\text{En}_{ss}}{(Mg_2Si_2O_6)_{opx}} \rightleftharpoons \underset{\text{En}_{ss}}{(Mg_2Si_2O_6)_{cpx}} \qquad (K_w', \Delta H_w, \Delta S_w, \Delta V_w)$$

and the Al-solubility of pyroxenes in equilibrium with an Al-phase

$$\underset{\text{En}_{ss}}{MgAl_2SiO_6} + \underset{\text{Ol}}{Mg_2SiO_4} \rightleftharpoons \underset{\text{Sp}}{MgAl_2O_4} + \underset{\text{En}_{ss}}{Mg_2Si_2O_6} \quad \text{(spinel facies)}$$

or

$$\underset{\text{En}_{ss}}{MgAl_2SiO_6} + \underset{\text{En}_{ss}}{Mg_2Si_2O_6} \rightleftharpoons \underset{\text{Gt}}{Mg_3Al_2Si_3O_{12}} \quad \text{(garnet facies)} \qquad (K_a', \Delta H_a, \Delta S_a, \Delta V_a)$$

The expressions for the various partition coefficients K' are discussed in a later section. Within the precision of the data, enthalpy and entropy are constant and the change in volume can be expressed as a function of the composition through:

$$\Delta V = v' + v''\ln K'$$

where v' and v'' are constant for a given reaction.

Considering the equilibrium reactions given above, one may write the system of equations

$$P = (RT \ln K_a' + T\Delta S_a - \Delta H_a)/(v_a' + v_a'' \ln K_a')$$

$$P = (RT \ln K_w' + T\Delta S_w - \Delta H_w)/(v_w' + v_w'' \ln K_w')$$

Combining these two equations yields independent temperature and pressure equations:

$$T(R \ln K_a' + \Delta S_a)(v_w' + v_w'' \ln K_w') - \Delta H_a(v_w' + v_w'' \ln K_w') = T(R \ln K_w' + \Delta S_w)(v_a' + v_a'' \ln K_a') - \Delta H_w(v_a' + v_a'' \ln K_a')$$

and

$$P(R \ln K_a' + \Delta S_a)(v_w' + v_w'' \ln K_w') + \Delta H_w(R \ln K_a' + \Delta S_a) = P(R \ln K_w' + \Delta S_w)(v_a' + v_a'' \ln K_a') + \Delta H_a(R \ln K_w' + \Delta S_w)$$

which can be rewritten as:

$$T = [\Delta H_a(v_w' + v_w'' \ln K_w') - \Delta H_w(v_a' + v_a'' \ln K_a')] / [(R \ln K_a' + \Delta S_a)(v_w' + v_w'' \ln K_w') - (R \ln K_w' + \Delta S_w)(v_a' + v_a'' \ln K_a')]$$

and

$$P = [\Delta H_a(R \ln K_w' + \Delta S_w) - \Delta H_w(R \ln K_a' + \Delta S_a)] / [(R \ln K_a' + \Delta S_a)(v_w' + v_w'' \ln K_w') - (R \ln K_w' + \Delta S_w)(v_a' + v_a'' \ln K_a')]$$

For simplification, the dimensionless denominator common to both equations will now be designated by D. The equations can be further simplified since $v_a'' = 0$ in all cases (Table 1), and they may be rewritten as functions of the actual variables $\ln K_a'$ and $\ln K_w'$:

$$T = [(v_w''\Delta H_a) \ln K_w' + (v_w'\Delta H_a - v_a'\Delta H_w)]/D$$

and

$$P = [(R\Delta H_a) \ln K_w' - (R\Delta H_w) \ln K_a' + (\Delta H_a \Delta S_w - \Delta H_w \Delta S_a)]/D$$

where

$$D = (v_w''R) \ln K_w' \cdot \ln K_a' + (v_w''\Delta S_a - v_a'R) \ln K_w' + (v_w'R) \ln K_a' + (v_w'\Delta S_a - v_a'\Delta S_w)$$

By dividing all the coefficients by $v_w''R$, these expressions become:

$$T = (t_1 \cdot \ln K_w' + t_2)/D$$

TABLE 1. Enthalpy, entropy, and change-in-volume data for enstatite–diopside and Al-pyroxene–Al-phase systems*

	-ΔH	-ΔS	-ΔV v'	-ΔV v"
	cal/mol	cal/mol/°K	cal/kb	cal/kb
En/Di	25195	14.15	80.62	35.68
Al-En/Sp	12535	7.31	168.0	0.
Al-Di/Sp	14977	9.80	220.0	0.
Al-Px/Gt	6295	2.79	171.4	0.

* *ΔV is approximated by a linear function (v' + v" lnK').*

and

$$P = (p_1 \cdot \ln K_w' + p_c \cdot \ln K_a' + p_2)/D$$

where

$$D = \ln K_w' \cdot \ln K_a' + d_1 \cdot \ln K_w' + d_c \cdot \ln K_a' + d_2$$

The values for the various t, p, and d coefficients are calculated as follows:

$$t_1 = \Delta H_a/R$$

$$t_2 = (v_w'\Delta H_a - v_a'\Delta H_w)/v_w''R$$

$$p_1 = \Delta H_a/v_w''$$

$$p_c = \Delta H_w/v_w'' = 706 \text{ kbar} \quad \text{(from data in Table 1)}$$

$$p_2 = (\Delta H_a \Delta S_w - \Delta H_w \Delta S_a)/v_w''R$$

$$d_1 = \Delta S_a/R - v_a'/v_w''$$

$$d_c = v_w'/v_w'' = 2.26 \quad \text{(from data in Table 1)}$$

$$d_2 = (v_w'\Delta S_a - v_a'\Delta S_w)/v_w''R$$

The numerical value for these coefficients depends generally on the pyroxene and/or the facies considered (Table 2), with the exception of p_c and d_c, which are constant.

TABLE 2. Thermodynamic parameters for the temperature and pressure equations*

	d_1	d_2	t_1(°K)	t_2(°K)	p_1(kb)	p_2(kb)
Al-En/Sp	- 8.387	+25.218	-6308.5	+45449.	+351.32	+ 95.99
Al-Di/Sp	-11.098	+32.765	-7537.5	+61152.	+419.76	+493.49
Al-Px/Gt	- 6.208	+31.037	-3168.1	+53754.	+176.43	-264.90

* *Derived from data in Table 1.*

Pyroxene geobarometers

Whereas a single set of thermodynamic parameters (ΔH, ΔS, v' and v'') is needed to define the Ca solubility in either diopside or enstatite for either facies (spinel or garnet) as a function of pressure and temperature (Mercier and Carter, 1975), a specific set of parameters must be derived for each pyroxene phase and for each facies to completely define the Al solubility in pyroxenes.

For the spinel facies, the thermodynamic parameters for Al (En) derived from MacGregor's (1974) experimental data have been adopted *as a model* for the true Al solubility for the average natural pyroxene compositions characteristic of metamorphic lherzolites (*op. cit.*, Cr/(Al+Cr−Na) from 15 to 25 percent in diopside and from 7 to 11 percent in enstatite). The validity of this model will be tested in a later section. Al(Di) isopleths and equations were also obtained by plotting the Al content of diopsides equilibrated in the spinel facies, as a function of temperature (derived from the diopside composition) and pressure (from the enstatite composition).

For the garnet facies, the Al(En) experimental and theoretical isopleths available are all in accord with MacGregor's experimental data, once Wood and Banno's (1973) corrections are applied to account for solid solution effects. Unfortunately, isopleths could not be obtained for the coexisting diopsides as this was done for the spinel facies. Indeed, since the equivalent Al used in geobarometry is defined (Mercier and Carter, 1975) as:

$$A = (\mathrm{Al} + \mathrm{Cr} - \mathrm{Na})/2$$

(in atomic fractions for a 6-oxygen formula)

A is negative for many diopsides due to the acmite component which is needed for stoichiometry.

However, the unusual plot of $(\mathrm{Al} + \mathrm{Cr})_{di}/A_{en}$ against Na_{di}/A_{en} has proven to be a valuable tool for obtaining a geobarometer based on diopside compositions for the garnet facies. If Al(En) and Al(Di) isopleths had similar slopes with $A_{di} = k.A_{en}$ (where k is a constant) and if the pyroxenes contained no Fe^{3+}, the data plotted would fit a straight line of slope equal to 1, since, from the definition of A:

$$A_{en} = (\mathrm{Al} + \mathrm{Cr} - \mathrm{Na})_{di}/k$$

which can be rewritten as:

$$(\mathrm{Al} + \mathrm{Cr})_{di}/A_{en} = k + \mathrm{Na}_{di}/A_{en} \qquad (\text{slope} = 1)$$

If the isopleth slopes were different for the two pyroxenes, for a given Na content a range of $(\mathrm{Al} + \mathrm{Cr})_{di}/A_{en}$ values would be obtained and a large scatter observed for this plot (*e.g.* spinel facies, Fig. 2). If the jadeite/acmite ratio varied with Na content, no linear fit could be obtained; *a fortiori,* if acmite was suddenly appearing for Na-rich compositions, a change in slope should be observed.

Actual data plotted in Fig. 1 fit, with very limited scatter, a straight line of equation

$$(\mathrm{Al} + \mathrm{Cr})_{di}/A_{en} = 2. + 0.82\ \mathrm{Na}_{di}/A_{en}$$

or

$$A_{en} = (\mathrm{Al} + \mathrm{Cr} + 0.82\ \mathrm{Na})_{di}/2.$$

By redefining the equivalent Al value for diopsides (at least in the garnet facies) as $(\mathrm{Al} + \mathrm{Cr} - 0.82\ \mathrm{Na})/2$, one concludes that both slopes and origins for the Al(En) and Al(Di) isopleths in the garnet facies are practically identical since, within the precision of the data, A_{en}/A_{di} becomes equal to unity. Therefore, for this facies, we may use the entropy, enthalpy, and change-in-volume data determined for the enstatite, if A is computed to take into account the minimum trivalent Fe present in diopside ($Fe^{3+}_{min} = 0.18\mathrm{Na}$).

Whereas the jadeite/acmite ratio remains prac-

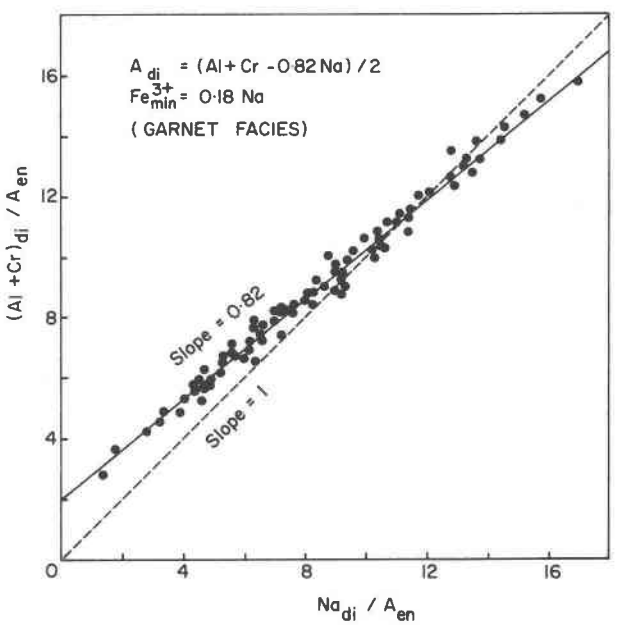

FIG. 1. Al+Cr *vs.* Na for diopsides equilibrated in the garnet facies. The normalization to A_{en} limits the scattering due to pressure or temperature effects and allows one to derive the empirical A_{di} expression taking into account Fe^{3+}. Data points below the dashed line correspond to pyroxenes for which Fe^{3+} is needed for stoichiometry. Data are from Nixon (1973), Boyd (1974), Ahrens *et al.* (1975) and include a few new analyses.

tically constant (jd/ac = 4.56) and independent of the Na content for diopsides in the garnet facies, there is no indication that this is true for the enstatite or that a similar relationship still holds in the spinel facies (or in the feldspar one) for which, on a similar plot (Fig. 2) more scatter is observed, in agreement with the distinct slopes found for the isopleths (Mercier and Carter, 1975). The steep fit obtained here is primarily due to a progressive enrichment in Na towards shallower levels of the mantle (behavior opposite to that of the garnet peridotites) until feldspar may form, then strongly depleting the diopside of its jadeite component.

Computation of the coefficients K_a' *and* K_w'

Mercier and Carter (1975) have derived, on a theoretical basis, the following expressions for the partition coefficients K_a' and K_w' for both facies,
—for the spinel facies,

$$K_w' = (1 - 2W_d)/(0.650 + 0.700W_d) = 5.714W_e/(1 - 2W_e)$$

$$K_a' = K_s'' \cdot A/(1 - A)$$

—for the garnet facies,

$$K_w' = (1 - 2W_d)/(0.862 + 0.276W_d) = 14.493W_e/(1 - 2W_e)$$

$$K_a' = K_g'' \cdot A \cdot (1 - A)$$

where the subscripts d and e refer respectively to diopside and enstatite, and where K_s'' and K_g'' are correction factors to account for major solid-solution effects. In both facies,

$$W = \mathrm{Ca}/(\mathrm{Ca} + \mathrm{Mg} + \mathrm{Fe}^{2+} + \mathrm{Mn})$$

and

$$A = (\mathrm{Al} + \mathrm{Cr} - n \cdot \mathrm{Na})/2$$

where the element symbols represent atomic fractions for 6-oxygen formulae.

Although Na is generally entirely ascribed to a jadeite component (*op. cit.*), the constant jadeite/acmite ratio (4.56) observed for diopsides in the garnet facies might also characterize the coexisting enstatite or both pyroxenes in the spinel facies. However, the Al/Na ratio for these pyroxenes is usually so large that the estimates are not really affected by the model chosen (n = 1 or 0.82). The effect of Fe^{3+} on the constants **f** = Di(Opx)/En(Cpx) (Fig. 3) is even too small (*e.g.* 0.139 instead of 0.138 for the garnet facies) to yield any appreciable change in the coefficients of the K_w' expressions.

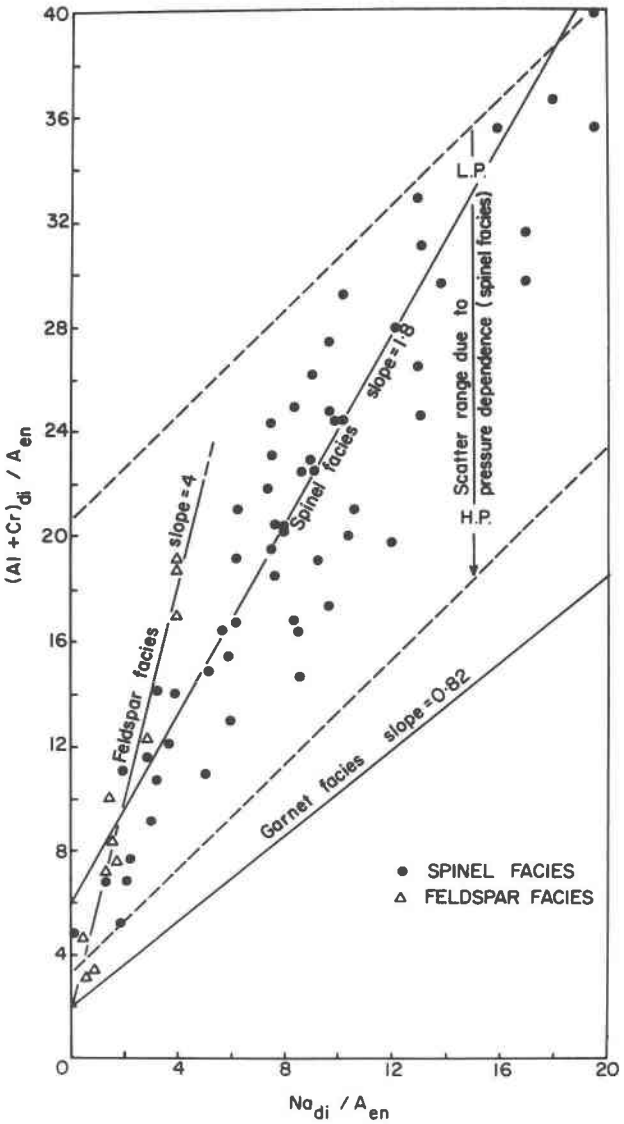

FIG. 2. Al+Cr *vs.* Na for diopsides equilibrated in spinel and feldspar facies. Even after normalization to A_{en}, an increase in pressure of equilibration lowers (Al+Cr) for a constant Na, indicating a stronger pressure of dependence of Al for diopside. Accordingly, Al(Di) isopleths (Mercier and Carter, 1975) are steeper. The large slopes observed prevent any inference about the existence and/or amount of Fe^{3+} contained in those pyroxenes. Data are from Ross *et al.* (1954), White (1966), Kutolin and Frolova (1970), Griffin (1973) and include new analyses.

On the other hand, as originally pointed out by Wood and Banno (1973), the Fe^{2+} content of the pyroxene may have an important effect on the Al concentrations observed at a given pressure. For the garnet facies, the correction factor,

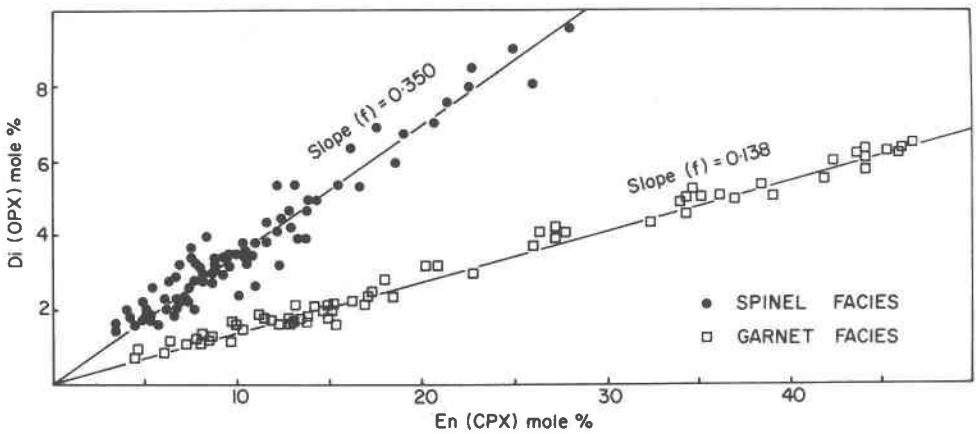

FIG. 3. Di(Opx) as a function of En (Cpx). The relation appears linear and independent of pressure or temperature for both facies. The precision is the same for both fits (σ = 0.007 or ± 10°C on the temperature estimate). Data from garnet pyroxenites equilibrated in the spinel–lherzolite facies (ariegites) are omitted, and would plot in intermediate positions. Mercier and Carter's (1975) original scale was erroneous and is now corrected. Data as in Figures 1 and 2.

$$K_g'' = (X_{Mg}^{M1})(X_{Mg}^{M2})^2/(1 - A)(X_{Mg}^{gt})^3$$

may be computed from the chemistry of enstatite[1] and coexisting garnet. Mercier and Carter (1975) showed that the garnet composition could be inferred with sufficient precision from the enstatite analysis only, thus allowing a similar correction to be made for xenocrysts, as the Fe/Mg partitioning between pyroxenes and garnet depends mainly on temperature and bulk composition. The correction has the effect of reducing both temperature and pressure, and therefore true corrected estimates are obtained only through an iteration readjusting alternatively temperature, pressure, and correction factor. The isopleths presented here (Fig. 4A, B) show the definitive K_g'' values derived from enstatite in both cases, plotted as functions of $-\ln K_w'$ and total Mg (atomic fraction) for either pyroxene:

$$K_g'' = 6.004 - 3.025\ \mathrm{Mg} + 0.702 \ln K_w' \quad \text{(enstatite)}$$

$$K_g'' = 3.298 - 1.781\ \mathrm{Mg} + 0.128 \ln K_w' \quad \text{(diopside)}$$

[1] The pyroxene structural formula is obtained as follows:
—Ca, Na and Mn in M2; Ti and Cr in M1.
—Fe^{3+} in M1 (either 0.18 Na or 0); $Fe^{2+} = Fe - Fe^{3+}$.
—$X_{Al}^{M1} = (Al - Fe^{3+} - Cr + Na)/2 - Ti$; $X_{Al}^{T} = Al - X_{Al}^{M1}$.
—$X_{Fe^{2+}}^{M1} = Fe^{2+}\ (T - 400)/3000$; $X_{Fe^{2+}}^{M2} = Fe^{2+} - X_{Fe^{2+}}^{M1}$.
—Mg is then distributed to obtain $X_i^{M1} = X_j^{M2}$.
This formula is consistent with either expression used for A. The partition coefficient for Fe is approximated for the range of temperatures dealt with from Virgo and Hafner's (1969) experimental data and Wood and Banno's (1973) model.

Mercier and Carter (1975) gave a similar theoretical expression for the correction factor K_s'' (spinel facies) and the corrections were negligible since K_s'' was generally close to 1 for natural peridotites. However, only divalent-cation effects were investigated and, as shown by MacGregor and Basu (1976), the effect of Cr solid solutions may be very important. Cr [or actually Cr/(Cr + Al − Na)] isopleths were constructed in $-\ln K_w'/A$ space for pyroxenes from a series of localities. The Cr isopleths were found to be practically parallel to the $-\ln K_w'$ axis and K_s'' was tentatively considered as a function of Cr only, for the common range of A values. A similar result is obtained by MacGregor and Basu (1976) as their Cr isopleths for spinel, in P-T space, are parallel to MacGregor's (1974) Al isopleths for pure aluminous enstatite. Considering the relationship illustrated in Figure 4C,

$$Cr/(Cr + Al + Fe^{3+})_{sp} = Cr/(Cr + Al - Na)_{di} = 2.2\ Cr/(Cr + Al - Na)_{en}$$

the following empirical correction factors are proposed:

$$K_s'' = 0.9 + 2.84\ (Cr/A)^3 \quad \text{(enstatite)}$$

$$K_s'' = 0.9 + 1.29\ (Cr/A)^3 \quad \text{(diopside)}$$

Tests and applications

Before applying the above technique to solve geological problems for which fresh 4-phase ultramafites are not available, one has to determine that (1) the Al

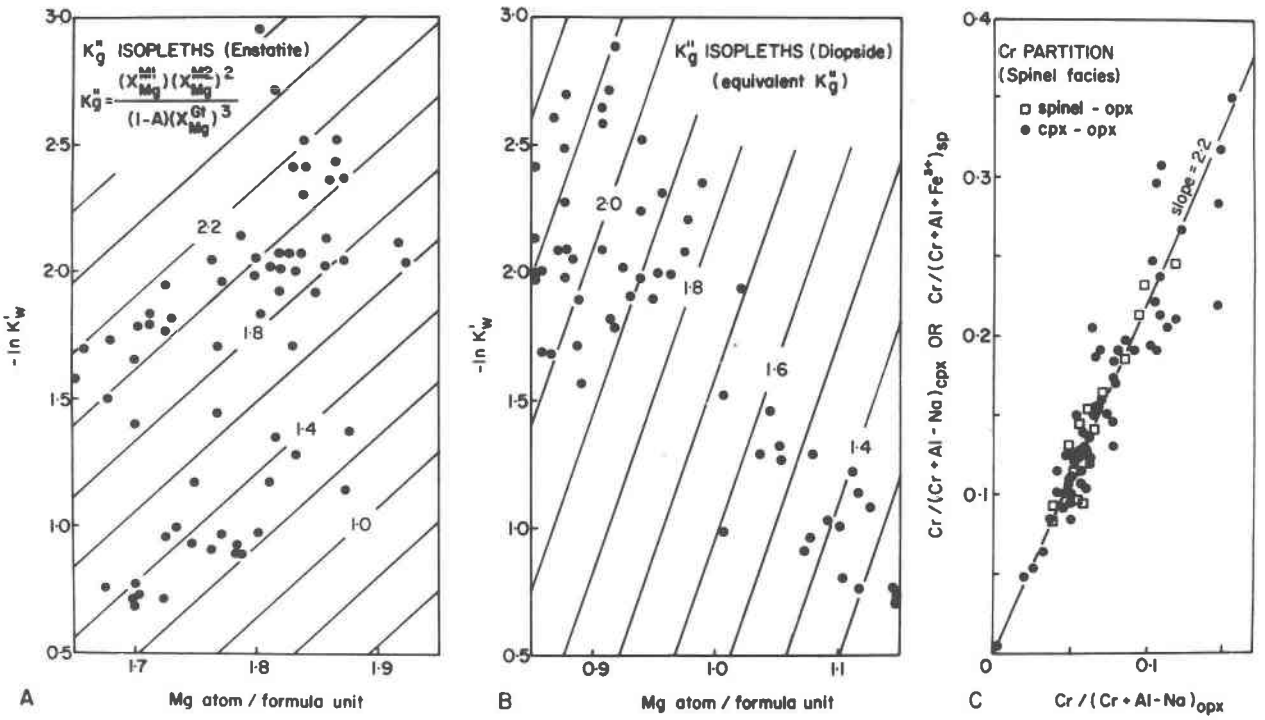

FIG. 4. K_g'' correction factors (garnet facies) and Cr partition (spinel facies). Data sources as in Figures 1 and 2. (A) K_g'' for enstatite as a function of $-\ln K_w'$ and Mg, respectively mainly dependent on temperature and bulk composition. K_g'' plotted is the definitive value after iteration. (B) K_g'' for diopside. K_g'' plotted has been actually computed from the coexisting enstatite composition. (C) Cr partition coefficients between enstatite and diopside or spinel for natural spinel peridotites.

solubility model for pyroxenes equilibrated in the spinel facies is valid, and (2) the precision to which the pressure and temperature estimates are made is not lowered when using the single-pyroxene techniques.

Verification of the method

A sequence of xenolith textures may be defined for any Vesuvian volcano, and through the comparison of over 150 xenolith associations they are grouped into four categories, each one assumed to represent a type of section through the upper mantle where basaltic magmas are generated. Among these various types, one is highly metasomatized and intruded by abundant pyroxenitic veins, and another is characterized by dominant blastogranular to blastolaminar textures,[2] and is systematically associated with major lithospheric shear-zones (*e.g.* Baja California, Pyrénées). The last two types of sequences, referred to as Borée (France) and Kilbourne (Kilbourne Hole, New Mexico) types, are texturally equilibrated metamorphic lherzolites with a log-normal grain-size distribution (homogranular textures) for all the silicate phases. Samples from these last two sequences are therefore regarded as illustrating steady-state flow in the upper mantle.

The Borée and Kilbourne types of sequences have no identical textural facies in common. However, a similar grain-size is observed at any depth (Fig. 5), and this grain size increases regularly with depth, in agreement with the conclusions previously drawn from the study of xenolith associations (Mercier, 1972). The depth range obtained in this study for Kilbourne Hole samples (25–60 km; Fig. 5) is in good agreement with that previously inferred from the petrology (equilibrium conditions between the xenoliths and host lava; MacGregor, 1970). The very high pressure estimates obtained from the high-temperature peridotites from the Boree-type sequence are not incompatible with a spinel-facies equilibrium; indeed, the exceptionally high bulk Cr/(Cr + Al) ratio (over

[2] These textures have been described as "porphyroclastic" by Mercier and Nicolas (1975). However, this early name appears now semantically incorrect (J. D. Blacic, pers, comm., 1975) and its replacement by "blastogranular" (or by "blastolaminar" for the most highly sheared facies) is suggested to permit standardization of the textural nomenclature. Alternatively, one might consider these textures as porphyroclastic subtypes (Mercier, 1972).

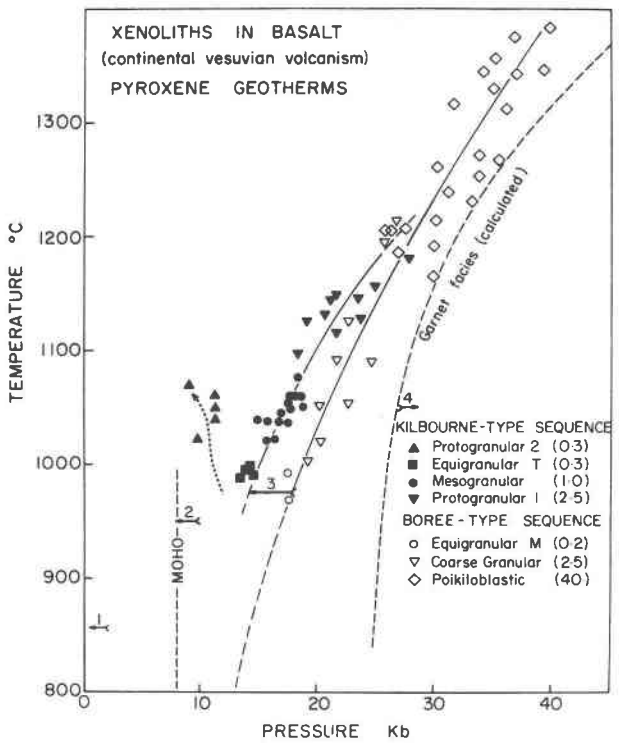

FIG. 5. Pyroxene geotherms for Borée-type and Kilbourne-type upper mantle sections, documented by xenoliths from Vesuvian volcanoes (new analyses). These xenoliths are texturally equilibrated and illustrate steady-state flow. The mean grain sizes (for olivine in the case of the poikiloblastic texture) are indicated in millimeters following the name of the textures. The data are for samples from Borée (France) and Black Rock Summit (Nevada) for the Borée-type sequence, and from Kilbourne Hole (New Mexico) and Cerzat (France) for the Kilbourne-type sequence. The arrows indicate the maximum uncertainty due to the model adopted, for (1) Kauai, Hawaii; (2) Dish Hill, California, and Beaunit, France (Moho.); (3) Frank Smith, South Africa (Moho.); (4) Frank Smith, South Africa (sp/gt facies boundary). Spinel garnet facies boundary calculated as for Figure 11. Data as in Figures 1 and 2.

1/3, inferred from the mineral compositions) shifts the spinel/garnet facies boundary to relatively higher pressures (MacGregor, 1970).

Plots of either temperature or pressure determined from one pyroxene, against that obtained from the second one (Fig. 6), for apparently equilibrated assemblages, illustrate the degree of confidence attained with this technique ($T \pm 30°C$; $P \pm 3$ kbar) for either spinel or garnet facies. Although exceptionally large discrepancies are considered as an indication of disequilibrium, in which case the error made by using the classical methods is several times the standard deviation given above, systematic divergence could also indicate analytical problems.

Inclusions from the Navajo Reservation "kimberlites"

The "kimberlites" from the Navajo Indian Reservation (Utah–Arizona; near Four Corners) have been studied by many (*e.g.* O'Hara and Mercy, 1966; McGetchin and Silver, 1970) for their xenoliths and/or xenocrysts. However, they do not have most of the characteristics of true South African kimberlites, such as penetrative serpentinization of both lava and inclusions, abundant metamorphic garnet–lherzolite xenoliths, pyroxene–ilmenite intergrowth nodules, *etc.* They are more comparable to European basaltic diatremes (Mercier, 1972), although the Navajo Reservation diatremes contain abundant pyrope xenocrysts, rarer crystals of clino- and orthopyroxenes, amphiboles, serpentine, and (limited to the southern diatremes; Fig. 7) abundant olivines. Shoemaker (1956) recognized a northeastern minette province in which occur the "kimberlites," and a monchiquite province restricted to the Hopi Buttes area. Whereas the monchiquite contains no deep-crustal or mantle xenoliths, the minette has abundant deep-crustal inclusions and rare peridotites (*e.g.* at Ship Rock; Baldridge *et al.*, 1975), and the "kimberlites" offer abundant xenoliths of both types. As is commonly observed, the "kimberlites" are associated with a dome structure of the basement, evidenced (Fig. 7) by the curvature of the restored Pliocene structural surface, which is interpreted as illustrating post-Pliocene magmatic activity, at least at depth.

The lherzolite xenoliths (hundreds of samples) apparently fall into two distinct petrographic suites, the highly hydrated peridotites which never contain fresh brown picotite and are commonly transformed into an aggregate of chlorite, amphibole, magnetite, and chromite, and the fresh spinel lherzolites similar to those found in many basaltic volcanoes (Mercier and Nicolas, 1975). Smith (1974, 1975) noticed some slight differences in composition, implying differences in equilibration conditions, for these two groups; however, new data (Fig. 8) show a complete overlap for the equilibration conditions of both series. Pyroxene xenocryst compositions yield a rather well-defined oceanic-type geotherm (Fig. 8), ignoring a few diopsides (dots in figure) on the basis of their magmatic origin inferred from Ti/Cr plots (Fig. 9). Equilibration conditions derived from the lherzolites generally yield much lower pressures, even crustal conditions (Fig. 8), and temperatures often well above the normal geotherm.

One hydrated peridotite still contains a large (0.4

mm) garnet crystal surrounded by a thick and complex kelyphite corona including remnants of a K1-type kelyphite (Lasnier, 1972; MK in Figs. 8 and 9) later reequilibrated (K2, K3), the last event being a general chloritization. The bulk composition of pyroxene inclusions in this garnet agrees with an original shallow garnet-facies or ariegite-subfacies equilibrium. No realistic pressure and temperature estimates were derived for pyroxenes in this peridotite or in most of the other samples by assuming a garnet-facies equilibrium and by applying the correction for either true garnet composition or that derived from the pyroxene chemistry. Neither of these peridotites can be regarded as metamorphic garnet lherzolites comparable to those from South Africa or from other American kimberlites. This is also supported by garnet factor analysis (Fig. 10). Whereas the crystals from metamorphic lherzolites, depleted or not, have a factor-8 value above 95 (Mercier, 1976a), in the present case the maximum value obtained (86) is still typical of magmatic ultramafic parageneses. Analyses of selected garnets most likely to have come from lherzolites on a color basis, together with dozens of analyses from the literature, have been processed in a vain attempt to find evidence for deep upper-mantle inclusions. The Ti and Cr concentrations observed are in accord with the results from factor analysis, with the exception of one xenocryst presently not understood. The garnet peridotite described above, thus, may be either a metasomatized garnet–lherzolite largely reequilibrated in the spinel facies (*e.g.* Eglazines; Mercier, 1972) or a spinel lherzolite in which ariegitic material has been mechanically scattered (*e.g.* Ronda, Beni Bouchera; Le Bois des Feuilles; Lasnier, 1972).

The conditions for reequilibration into the present hydrous phases must have been reached fast enough to quench most of the original assemblages, as some hydrated xenoliths may still have pyroxenes equilibrated in the garnet facies, but also slow enough to allow partial reequilibration in intermediate conditions (K1-type kelyphite). Therefore, the peridotite emplacement into shallow levels is not related to any volcanic event but to a slower tectonic phenomenon, and the temperature–pressure trend observed would correspond to an equilibrium situation (geotherm) and not to a requilibration path. The actual present equilibration conditions are much shallower than inferred from geobarometry; thick serpentine veins formed continuously before and after deformation events in high-pressure-facies rocks. An *in situ* diapiric intrusion of upper-mantle material in crustal regions would explain this second geotherm and the hydration and the quasi-absence of sheared facies only with difficulty, and would not be supported by any tectonic evidence. However, Helmstaed and Doig's (1975) model, which considers the C-type eclogites so abundant in the Navajo Reservation dia-

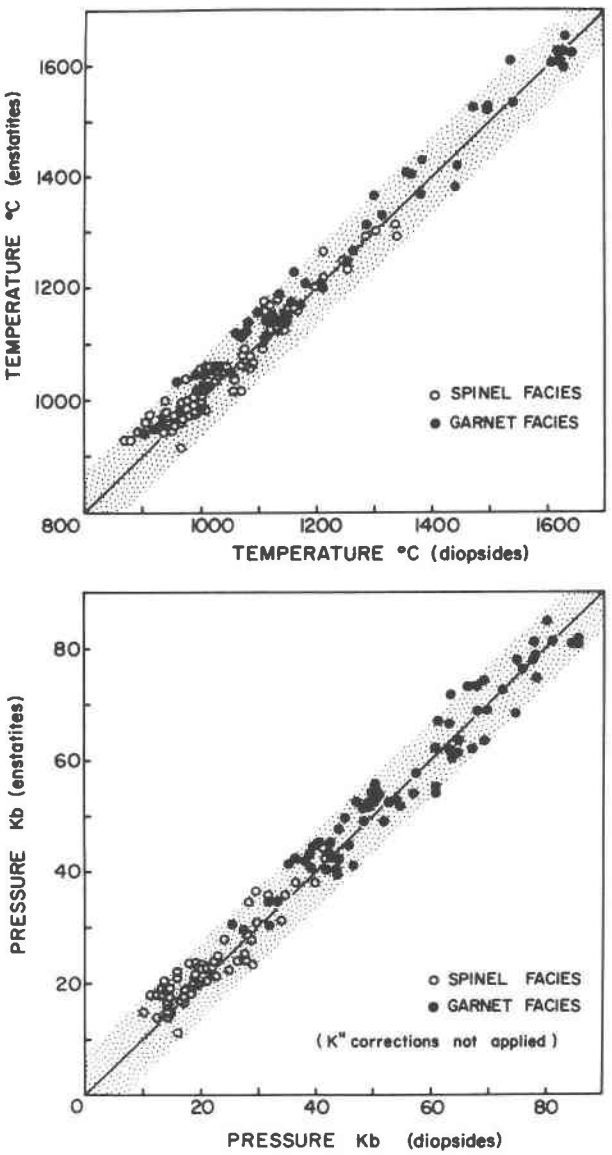

FIG. 6. T/T and P/P plots for estimates derived independently from enstatite and diopside in equilibrated assemblages. The estimates are not corrected for solid solution effects in this particular plot. No systematic deviation has been observed at any pressure indicating that **f** (Fig. 3) is dependent on the nature of the Al-phase rather than on the pressure itself. The precision for temperature and pressure estimates is respectively ± 30°C and ± 3 kbar, assuming ideal thermodynamic parameters and standard quality analyses. Data as in Figures 1 and 2.

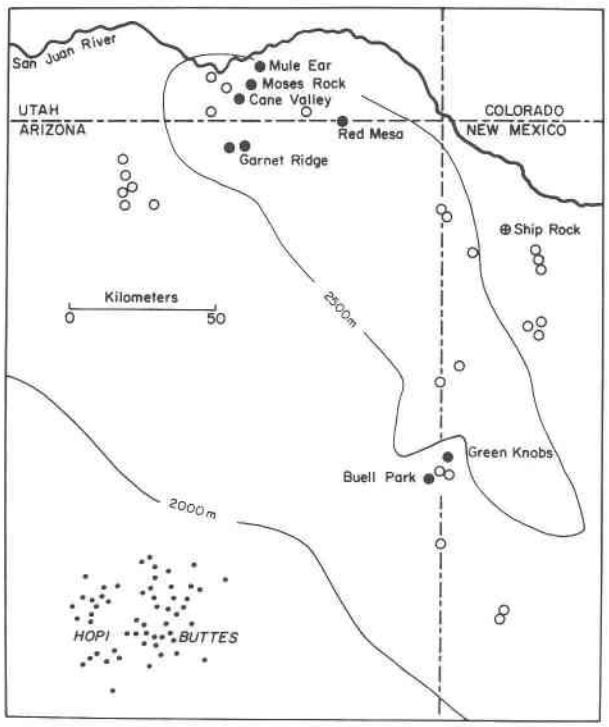

FIG. 7. The volcanics of the Navajo Indian Reservation, near Four Corners: monchiquite (dots), minette (open circles) and "kimberlites" (solid circles). The contours are for the restored Pliocene surface (modified after Shoemaker, 1956).

tremes as metamorphosed underthrust oceanic crust, provides a satisfactory model for the hydrated peridotites as quenched "ophiolitic" slices characterized by a typical oceanic paleogeotherm (also in agreement with the textures). In any case, the actual geotherm beneath the Navajo Reservation would be of oceanic type, and the diatremes present no evidence whatsoever for a genesis at depths comparable to those for kimberlites. These garnet-rich diatremes are therefore regarded as minette-type magmas which originated in the shallower zones of the garnet facies and were contaminated as they passed through highly hydrated ultramafites and eclogites. This interpretation also agrees with the close field association of minettes and "kimberlites."

Western Newfoundland ophiolites

The Newfoundland ophiolites of the Western Platform (Fig. 11, inset) have been recently interpreted as obducted slices of lithosphere from a Cambrian basin (Mercier, 1976b) on the western side of the Eocambrian-Cambrian Iapetus (or Proto-Atlantic Ocean; Dewey and Bird, 1971). Because of the intensive serpentinization and/or recrystallization of most of the sequence, the technique described above has been used, yielding a remarkably high thermal gradient, even for oceanic lithosphere. The pyroxene geotherm derived (Fig. 11) is defined for a pressure range of almost 40 kbar, much larger than expected from the reconstructed structural section (8 kbar). Since the possible errors due to the Al-solubility model adopted (Fig. 5) are far smaller than the discrepancies observed between the pyroxene geotherm and the structural section, the latter must have been shortened during obduction.

From the gabbros (top) to the metamorphic aureole (base), the ultramafic sequence comprises cumulate wehrlites and dunites, sheared (porphyroblastic) metamorphic dunites, protogranular harzburgites, and sheared (blastolaminar) lherzolites. The protogranular harzburgites exist within a depth range equivalent to a few kilobars, in agreement with the section, but their equilibration at greater depths indicates an intensive shortening of the shallower

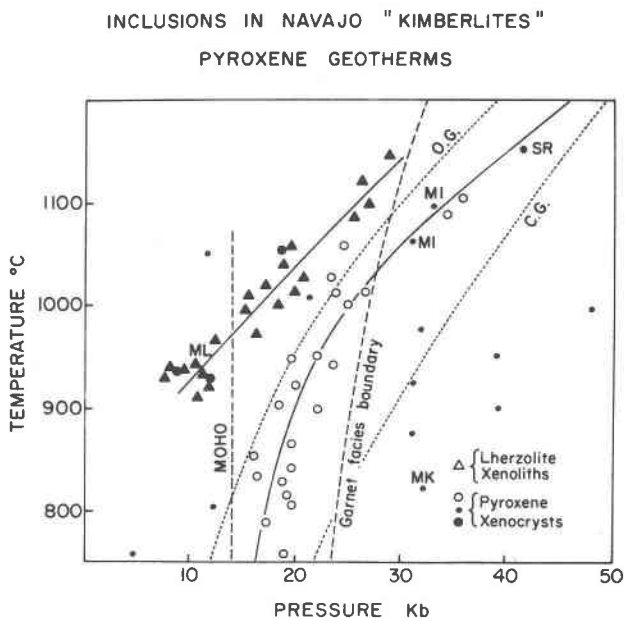

FIG. 8. Pyroxene geotherm derived from the pyroxene xenocrysts in the Navajo "kimberlites." A second trend at higher temperature and lower pressure corresponds mainly to the lherzolite xenoliths, hydrated or not, plus some xenocrysts from Garnet Ridge. Abbreviations: SR = Ship Rock (Baldridge *et al.*, 1975); MI, MK, ML = Moses Rock garnet lherzolite MSS-1; respectively, inclusions in garnet, K1-pyroxene depleted in Al by surrounding K2-amphibole, and pyroxenes in lherzolite. Some of the data are from O'Hara and Mercy (1966), Watson and Morton (1969) and McGetchin and Silver (1970). The dotted lines correspond to the oceanic and continental geotherms of Mercier and Carter (1975). Spinel/garnet facies boundary as in Figure 11. Dots and open circles as in Figure 9.

dunites in accordance with their texture. Thus, rather than offering a continuous section through an oceanic lithosphere, these ophiolites are formed of at least two superposed sequences, as has also been observed in Quebec (Laurent, 1975). The basal sheared lherzolites, although presently a few hundred meters thick, correspond to a series originally more than 30 km thick. In this case, the shortening affected the entire formation, in agreement with the field observations of abundant fault zones subparallel to the original shear surface. The maximum depths observed are consistent with the ariegite subfacies in which the lherzolites were equilibrated. Reequilibration paths are also obtained for the basal lherzolites by comparing the estimates derived from the bulk compositions of relict crystals and neoblasts. The paths indicate a subhorizontal shear consistent with the early stage of obduction for the deepest lithospheric material. The drop in temperature (over 350°C) is explained by the original extraordinarily high thermal gradient, and by the change from an oceanic thermal regime to a continental one during the obduction process. The effects of stress on the enstatite–diopside join are likely to be negligible, as in some sheared peridotites (*e.g.* Lesotho, Mercier and Carter, 1975; Beaunit, Mercier, 1972) the deformation (variable strains) occurs without any simultaneous exsolution phenomenon in the pyroxenes, at least to the resolution of optical microscopes.

Conclusions

The method presented here for computation of pressure and temperature estimates from pyroxene compositions is more general than the classical one by which compositions are directly compared with the available experimental results. Furthermore, with the new evidence of pressure sensitivity of the enstatite–diopside solvi (Warner and Luth, 1974; Lindsley and Dixon, 1976), the determinations should be done through iterations, and more calculations are needed for correcting the estimates for solid-solution effects. The method proposed allows the direct computation of fully corrected estimates through the use of simple equations, even when the composition of all the coexisting phases are unknown. The equations are derived in such a way that any further refinement of either experimental data or empirical laws for natural assemblages can be taken into account by simply changing the appropriate coefficient.

Applications of this method are many and include the use of partially reequilibrated assemblages, altered facies, or xenocrysts for deriving conditions of equilibrations impossible to obtain by using any classical method. Further possibilities are the construction of pressure-temperature paths for partially recrystallized and reequilibrated textures, and also to

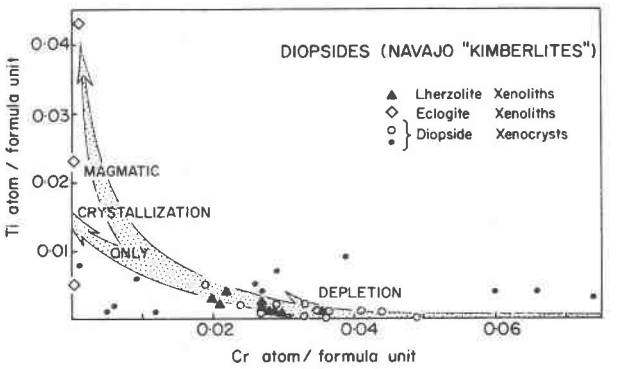

FIG. 9. Ti/Cr diagram for diopsides from the Navajo Country diatremes. On the basis of this diagram, only part of the xenocrysts (open circles) are likely to have been equilibrated in metamorphic four-phase parageneses (Mercier, 1976a).

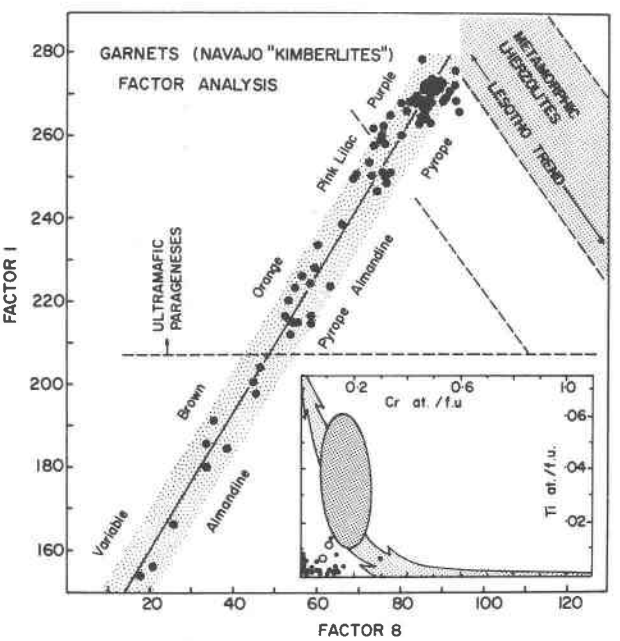

FIG. 10. Garnet factor analysis for the Navajo Country diatremes. Many different parageneses are represented by the variously colored garnets, but none can be related to metamorphic uppermantle material. Data sources as in Figure 8. Some other data are from Reid and Hanor (1970). Inset: Ti/Cr diagram for some of the garnet xenocrysts (Ti and Cr are given in atoms per formula unit). The same conclusion is reached, with the exception of one crystal. The open circles are for the Ship Rock and for the Moses Rock garnet–peridotites. Data sources as in Figure 8. The trends are for magmatic and metamorphic (depleted) mantle garnets (Mercier, 1976a). The field for the undepleted garnets is shown by the heavy pattern.

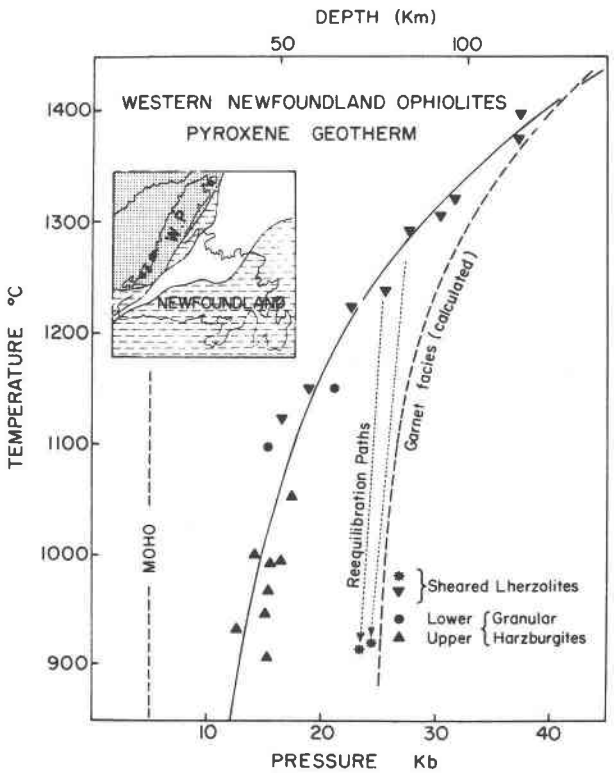

FIG. 11. Pyroxene geotherm for the obducted ophiolites of the Western Platform, Newfoundland (new analyses). The garnet-facies upper boundary is calculated from O'Hara *et al.*'s (1971) experimental data, corrected for friction, adjusted to Richardson *et al.*'s (1968) pressure scale and modified for the actual Cr/Al ratio after MacGregor's (1970) data. The depth of the Moho, for the Baie Verte basin is inferred from the geology. Asterisks are for reequilibrated neoblasts in blastogranular-textured samples. Inset: Location of the ophiolites (black) obducted onto the Canadian Shield (heavy pattern); also shown, the remnant Iapetus crust (no pattern; includes island-arc material) which has not been subducted (Mercier, 1976b).

check either the equilibrium state of a paragenesis or the quality of the analyses. The error on the estimates, assuming ideal experimental data, is less than 30°C and 3 kbar, and the maximum error may even decrease by one-third for superior analyses. In any case, using both pyroxene phases independently yields maximum and minimum values for the estimates instead of a single set of assumed equilibration conditions.

The geological examples just discussed show a few characteristics useful for a better understanding of the earth's upper mantle and its related tectonics. The grain-size of peridotite inclusions in basalts always increases with depth as a partial consequence of the elevation in temperature. However, the average grain-size at depths over 200 km is about the same as that of samples equilibrated at half this depth. These observations may give some clues about the mode of flow of the upper mantle, as the grain size is related mainly to the applied deviatoric stress, or alternatively to the temperature and strain rate (Carter and Mercier, 1976). The sheared peridotites might thus illustrate transient conditions resulting from a considerable increase in strain rate or stress, accompanied (Newfoundland, $\Delta T = 350°C$, $\Delta\sigma = 3$kbar; Mercier, 1976b) or not (Lesotho; Mercier and Carter, 1975) by a decrease in temperature, and possibly combined with minor effects of other physical or chemical parameters. Accordingly, these textures are dominant only for inclusions in basalts from active fault zones. Ophiolites, generally regarded as single slices of lithosphere on the basis of coherent and continuous structural sections, might rather be a series of smaller slices resulting from inhomogeneous strain, the deepest one having moved fastest, thereby producing a shortening of the original sequence. The data obtained for the inclusions from the Navajo Indian Reservation provide new evidence (other evidence being the abundance of C-type eclogites) in favor of complex upper-mantle tectonics, with possible underthrusting of oceanic material along enormous distances. In any instance, despite the abundance of pyrope xenocrysts, these volcanics, commonly referred to as "kimberlites," are not real kimberlite of deep origin.

Acknowledgments

The writer is indebted to Dr. S. N. Ehrenberg for making available unpublished analyses, to Dr. N. L. Carter and D. A. Anderson for critical comments and beneficial suggestions, and to C. Mercier for the illustrations.

This work was supported by National Science Foundation grant AO-31569-001.

References

AHRENS, L. H., J. B. DAWSON, A. R. DUNCAN AND A. J. ERLANK, Editors (1975) Papers presented at the First International Conference on Kimberlites. *Phys. Chem. Earth* **9**, 1–940.

BALDRIDGE, W. S., S. N. EHRENBERG AND T. R. MCGETCHIN (1975) Ultramafic xenolith suite from Ship Rock, New Mexico (abstr.). *EOS*, **56**, 464.

BOETTCHER, A. L. (1974) Review of symposium on deep-seated rock and geothermometry. *EOS*, **56**, 1068–1072.

BOYD, F. R. (1974) Ultramafic nodules from the Frank Smith kimberlite pipe, South Africa. *Carnegie Inst. Wash. Year Book*, **73**, 285–294.

CARTER, N. L. AND J-C. C. MERCIER (1976) Stress dependence of olivine neoblast grain sizes. (abstr.) *EOS*, **57**, 322.

DEWEY, J. F. AND J. M. BIRD (1971) Origin and emplacement of the ophiolite suite: Appalachian ophiolites in Newfoundland. *J. Geophys. Res.* **76**, 3179–3206.

GRIFFIN, W. L. (1973) Lherzolite nodules from the Fen alkaline complex, Norway. *Contrib. Mineral. Petrol.* **38**, 135–146.

HELMSTAEDT, H. AND R. DOIG (1975) Eclogite nodules from kimberlite pipes of the Colorado Plateau—samples of subducted Franciscan-type oceanic lithosphere. *Phys. Chem. Earth* **9,** 95–111.

KUTOLIN V. A. AND V. M. FROLOVA (1970) Petrology of ultrabasic inclusions from basalts of Minusa and Transbaikalian regions, Siberia, USSR, *Contrib. Mineral. Petrol.* **29,** 163–179.

LASNIER, B. (1972) Les péridotites et pyroxénolites à grenat du Bois des Feuilles, Monts du Lyonnais, France. *Contrib. Mineral. Petrol.* **34,** 29–42.

LAURENT, R. (1975) Occurrences and origin of the ophiolites of southern Quebec, northern Appalachians. *Can. J. Earth Sci.* **12,** 443–455.

LINDSLEY, D. H. AND S. S. DIXON (1976) Diopside–enstatite equilibria at 850°–1400°C, 5–35 kbar. *Am. J. Sci.* in press.

MACGREGOR, I. D. (1970) The effect of CaO, Cr_2O_3, Fe_2O_3 and Al_2O_3 on the stability of spinel and garnet peridotites. *Phys. Earth Planet. Inter.* **3,** 372–377.

——— (1974) The system MgO–Al_2O_3–SiO_2: Solubility of Al_2O_3 in enstatite for spinel and garnet peridotite compositions. *Am. Mineral.* **59,** 110–119.

——— AND A. R. BASU (1976) Geological problems in estimating mantle geothermal gradients. *Am. Mineral.* **61,** 715–724.

MCGETCHIN, T. R. AND L. T. SILVER (1970) Compositional relations in minerals from kimberlite and related rocks in the Moses Rock dike, San Juan County, Utah. *Am. Mineral.* **55,** 1738–1771.

MERCIER, J-C. C. (1972) Structures des péridotites en enclaves dans quelques basaltes d'Europe et d'Hawaii. Regards sur la constitution du manteau supérieur. *These Doct. 3e Cycle,* Nantes, France. 1–229.

——— (1967a) Petrochemical classification of peridotites. *Schweiz. Mineral. Petrogr. Mitt.,* in press.

——— (1976b) Newfoundland ophiolites and plate tectonics. *Tectonophysics,* in press.

——— AND N. L. CARTER (1975) Pyroxene geotherms. *J. Geophys. Res.* **80,** 3349–3362.

——— AND A. NICOLAS (1975) Textures and fabrics of upper-mantle peridotites as illustrated by xenoliths from basalts. *J. Petrol.* **16,** 454–487.

NIXON, P. H., Editor (1973), Lesotho Kimberlites. *Lesotho National Development Corporation, Maseru, Lesotho, South Africa.,* 350 p.

O'HARA, M. J. AND E. L. P. MERCY (1966) Eclogite, peridotite, and pyrope from the Navajo Country, Arizona and New Mexico. *Am. Mineral.* **51,** 336–352.

——— S. W. RICHARDSON AND G. WILSON (1971) Garnet-peridotite stability and occurrence in crust and mantle. *Contrib. Mineral Petrol.* **32,** 48–68.

REID, A. M. AND J. S. HANOR (1970) Pyrope in kimberlite. *Am. Mineral.* **55,** 1374–1379.

RICHARDSON, S. W., P. M. BELL AND M. C. GILBERT (1968) Kyanite-sillimanite equilibrium between 700°C and 1500°C. *Am. J. Sci.* **266,** 513–541.

ROSS, C. S., M. D. FOSTER AND A. T. MYERS (1954) Origin of dunites and of olivine-rich inclusions in basaltic rocks. *Am. Mineral.* **39,** 693–737.

SHOEMAKER, E. M. (1956) Occurrence of uranium in diatremes on the Navajo and Hopi reservations, Arizona, New Mexico and Utah. *U. S. Geol. Surv. Prof. Pap.* **300,** 179–185.

SMITH, D. (1974) Lherzolite inclusions from Green Knobs, McKinley County, New Mexico (abstr.). *Geol. Soc. Am. Abstr.* **6,** 1066.

——— (1975) Relative abundance, compositions and *P-T* histories of ultramafic xenoliths, Green Knobs, New Mexico, and implications for the mantle below the Colorado Plateau. (abstr.) *Geol. Soc. Am. Abstr.* **7,** 1275.

VIRGO, D. AND S. S. HAFNER (1969) Fe^{2+}–Mg order–disorder in heated orthopyroxenes. *Mineral. Soc. Am. Spec. Pap.* **2,** 67–81.

WARNER, R. D. AND W. C. LUTH (1974) The diopside- orthoenstatite two-phase region in the system $CaMgSi_2O_6$– $Mg_2Si_2O_6$. *Am. Mineral.* **59,** 98–109.

WATSON, K. D. AND D. M. MORTON (1969) Eclogite inclusions in kimberlite pipes at Garnet Ridge, Northeastern Arizona. *Am. Mineral.* **54,** 267–285.

WHITE, R. W. (1966) Ultramafic inclusions in basaltic rocks from Hawaii. *Contrib. Mineral. Petrol.* **12,** 245–314.

WOOD, B. J. AND S. BANNO (1973) Garnet–orthopyroxene and clinopyroxene–orthopyroxene relationships in simple and complex systems. *Contrib. Mineral. Petrol.* **42,** 109–124.